

Muography of a water-Cherenkov detector of the Pierre Auger Observatory

Catarina Felgueiras^{1,a} and Daniel Sousa^{1,b}

¹ *Universidade do Minho, Braga, Portugal*

Project supervisors: R. Sarmento and S. Andringa

November 1, 2022

Abstract. The goal of this work is the development of an analysis to reconstruct the energy spectrum of the muons based on simulation data that mimic the conditions of the fall of relativistic particles from the shower of particles that reach the tanks in the Pierre Auger Observatory and their detectors. We applied the muography technique to the observatory's tanks to explore different aspects of it. Although we don't get a full energy spectrum, we were able to recreate part of it and we can understand what aspects should be improved in order to achieve better results.

KEYWORDS: Muography, Energy Spectrum, Simulation, Pierre Auger Observatory

1 Introduction

1.1 Muons

Muons, fundamental subatomic particles, are highly penetrating charged particles that are produced from the interaction of the cosmic rays (mainly high-energy protons) with the atmosphere which creates particle showers. The muons collide with the Earth at a speed similar to the speed of light and have a flux on the ground that is well-known and constant. The lifetime of a muon in a static referential is $2,2 \mu\text{s}$ but for a speed similar to the speed of light occurs time dilation and the lifetime of a muon increase. These particles are similar to the electrons with the same charge, however, they have a higher mass that allows these particles to go through matter with little interaction, traveling great distances in a straight line before being stopped. As mentioned, a muon has some kinetic energy associated however when they go through the matter, the muon loses a quantity of energy that's equal to $2 \text{ MeV}/(\text{gcm}^2) \times \text{distance traveled (in cm)} \times \text{matter's density}$. This expression stands for the minimum energy of a muon that can pass through a piece of matter.

1.2 Muography

Muography is a modern technique that uses the muons and their characteristics for characterizing a structure. Also, we need detectors that reconstruct the muon's trajectory. It's known that the muons need to have the necessary energy to pass through the material and the energy that the muons lose is related to the distance that they travel and the material's density. It's expected that more muons will reach the detectors if they come from a direction where they go through less matter. By studying the absorption of the muon from certain directions, we can produce a projected image of a target volume, the muography. Basically, muography is similar to radiography but on a larger scale.

1.3 Pierre Auger Observatory

The Pierre Auger Observatory is located in Argentina, and it's the biggest installation whose main focus is the detection and study of the highest-energy particles in the Universe, which hit the Earth from all directions, so-called cosmic rays. The Auger Observatory is a hybrid detector, employing two independent methods to detect and study these particles. In our project, we focus only on one method that detects high-energy particles through their interaction with water placed in surface detector tanks. The tanks are full of water and have photomultipliers installed inside. In this case, when the muons pass through those tanks and interact with the water, they emit Cherenkov radiation. The photomultiplier sensors of the tank measure and convert this radiation into an electrical signal, and in this way, it is possible to detect the particles. Those tanks are cylinders with 12000 liters of capacity [1][2].

1.4 RPC's

Underneath a few tanks, there are 4 RPC's, Resistive Plate Chambers. They are gaseous resistive parallel plate avalanche detectors. The RPC's are divided into segments, the pads. Each RPC contains 64 pads (8 by 8) and each pad has the dimensions of 18 cm by 14 cm. When muons go through a pad, we are able to get the information from where the muons crossed the RPC because the gas is ionized, the applied electric field generates a current and there is induction of electric charge in the pad, see Figure 1 [3].

1.5 UMD

Under the tank, at 2.3 m depth there is a scintillator detector covering a total area of 30m^2 , which was designated UMD (Underground Muons Detector). This detector is divided in four rectangular modules. Two of these modules have 1/3 of total area each. The other two take 1/6 of the total area each.

^ae-mail: a100506@alunos.uminho.pt

^be-mail: a96083@alunos.uminho.pt

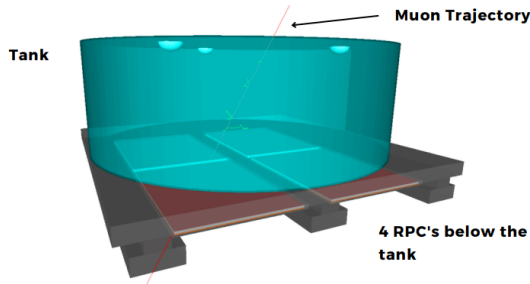


Figure 1. Structure Scheme of the tank in Pierre Auger Observatory.

1.6 Relevant variables

Here we present a list of the main variables which can be measured with the detector and are used in this analysis. It should be noted that we use natural units: $c = 1$.

- $m = 105.66 \text{ MeV}/c^2$: Muon Mass;
- p : Linear Momentum;
- p_x, p_y, p_z : Momentum Components;
- $E_k = \sqrt{m^2 + p^2} - m$: Kinetic energy of a muon;
- $\theta = \cos^{-1} \frac{p_z}{p}$: Zenith Angle;
- $\phi = \tan^{-1} \frac{p_y}{p_x}$: Azimuth Angle;
- $\tan \theta_x = \frac{p_x}{p_z}$;
- $\tan \theta_y = \frac{p_y}{p_z}$

2 Data

All the data used for the analysis came from simulations of the atmospheric particles at an altitude of 1400 m, imitating the conditions of the Observatory, with the following information for each particle found: particle type, the components of the moment, the position of arrival at the ground and subsequently the energy lost in the tank and underground by a particle in a given position, among other information irrelevant to our project. This simulation has 22996300 entries, of which 4667648 correspond to muons, and it is estimated to correspond to around 2 hours of atmospheric flux.

3 Muon Distributions

3.1 Energy Spectrum

Our main objective, as mentioned earlier, is to reconstruct the energy spectrum of muons from a particle shower. Our first step was based on building a spectrum of muon energy in simulation with all the information we had in our possession, shown in Figure 2. We reinforce that in a real situation we would not have information of the moment of the muons as we have in simulation and that allowed us to sketch this first spectrum.

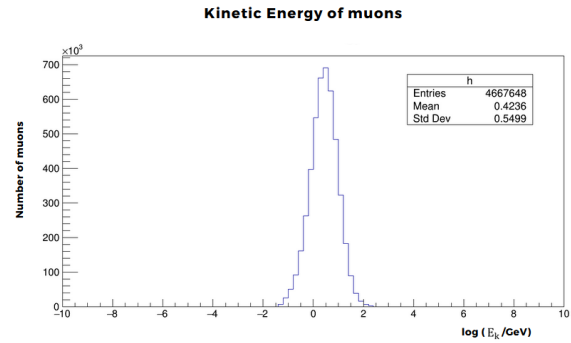


Figure 2. Kinetic Energy of the muons present in the simulation data.

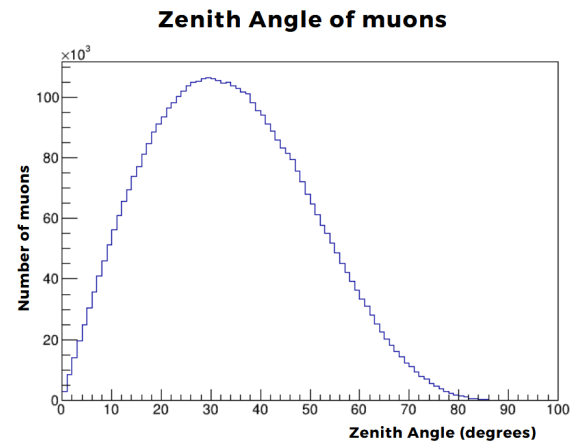


Figure 3. Zenith Angle of the muons.

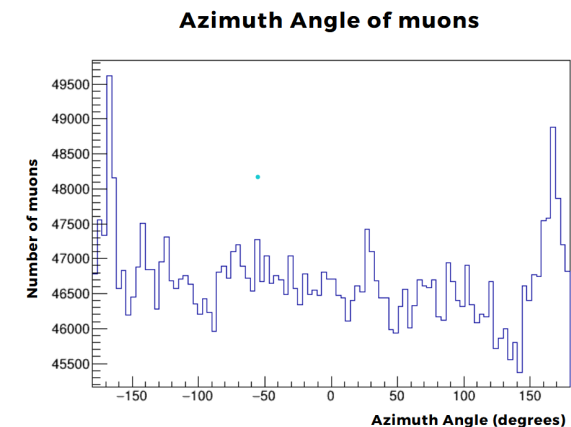


Figure 4. Azimuth Angle of the muons.

3.2 Angular Distributions

To study the direction of the muons and have a general idea of the directions of the more energetic particles, we built these two histograms. One represents the number of muons as a function of the zenith angle, Figure 3, and the other is similar, but concerns the azimuthal angle, Figure 4, with both angles in degrees.

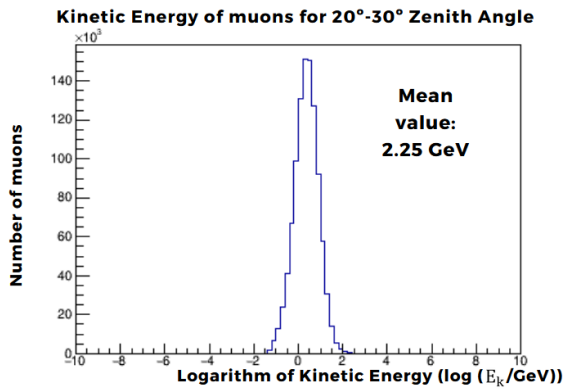


Figure 5. Energy Spectrum with a θ cut: 20°-30°.

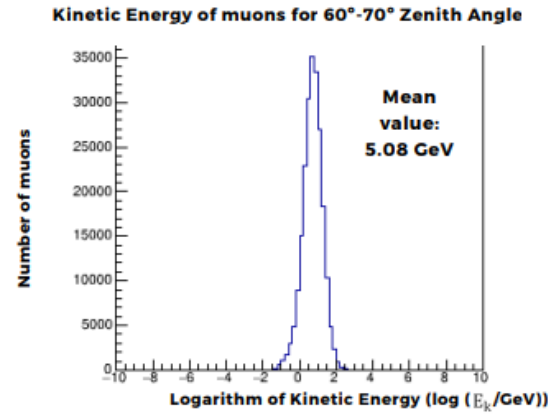


Figure 7. Energy Spectrum with a θ cut: 60°-70°.

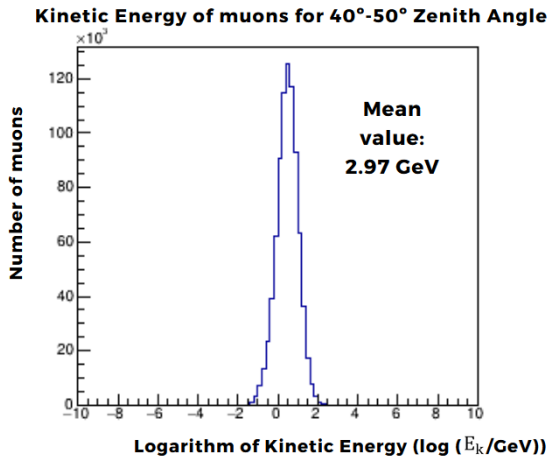


Figure 6. Energy Spectrum with a θ cut: 40°-50°.

Focusing on the first graph there is a peak for a 30° theta. The number of muons increases with the increase of theta just for a geometric reason - the solid angle increases with theta. However, for higher theta, it begins to decrease because the effect of the attenuation of the muons in the atmosphere begins to dominate. In the second graph, the variations present come from statistical fluctuations because, in this case, the muons, reach the earth's surface from all directions, without preference of any.

Continuing the analysis with the obtained data, we apply zenith angle cuts to the muon energy spectrum, Figures 5, 6 and 7, and verify that there is a shift to the right. The kinetic energy of the muons increases with the increase of the zenith angle, concluding that muons with more inclined directions have higher kinetic energy associated.

4 Muographies

4.1 Muography of the $\tan \theta_x$ and $\tan \theta_y$

We plot the tangent of theta x versus the tangent of theta y, first for all muons and then only for transmitted muons. Transmitted muons are understood to mean the muons that pass through the tank and the respective water inside until reaching the RPC's located below the tank. The muon

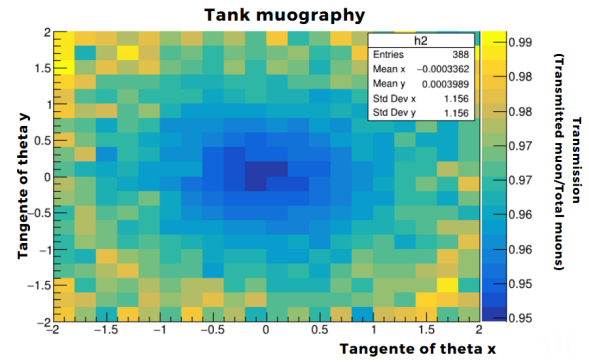


Figure 8. Muography of the tank.

is transmitted if its kinetic energy is greater than the energy lost along its trajectory: in the tank water and underground until it reaches the RPC. By dividing the transmitted muons by all muons, we arrive at a graph that partially indicates the direction of the transmitted muons, Figure 8. This procedure was made for all the muons in the sample.

The highest absorption rates are located in the center of muography, for very low $\tan \theta_x$ and $\tan \theta_y$. These directions correspond to muons with vertical trajectories. We conclude then that on average vertical muons pass through a greater amount of water in the tank, lose more energy (by the formula and explanation presented in the introduction), and are more absorbed. It should be noted that, contrary to expected because muons with inclined trajectories can cross a greater amount of water, there is a greater amount of these that crosses the RPC near the edge, then pass through a relatively small amount of water inside the tank.

4.2 Muography of the positions of the muons at the pads

Following the previous process, we have drawn the transmission histogram of the muons over the x and y coordinates and with the binning adjusted to the pads, shown in Figure 9.

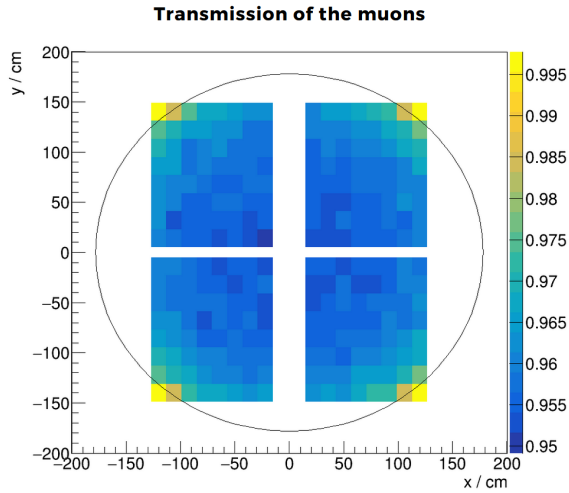


Figure 9. Muography of the tank (the circle corresponds to the limits of the tank).

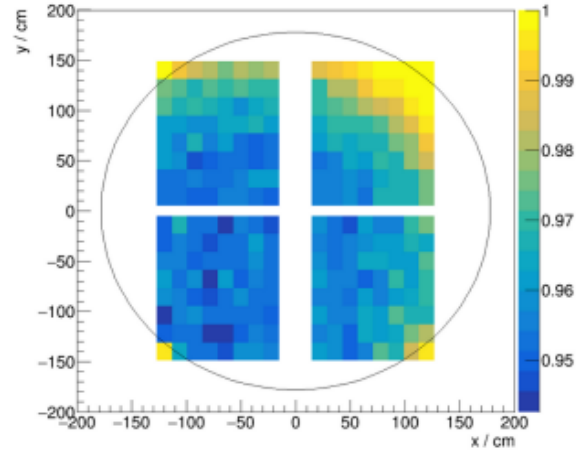


Figure 11. Muography of the tank with $\theta \in [30^\circ, 60^\circ]$ and $\phi \in [0^\circ, 90^\circ]$.

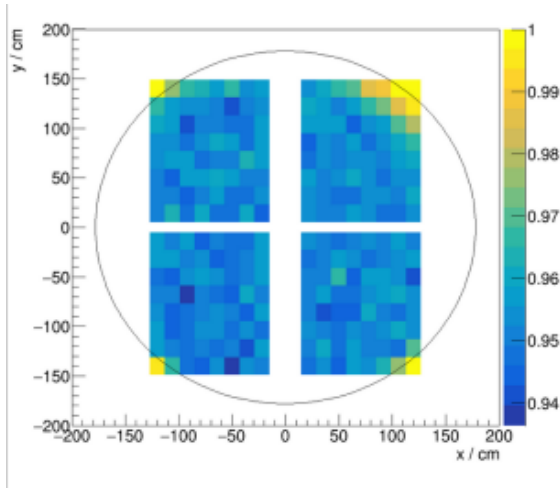


Figure 10. Muography of the tank with $\theta \in [0^\circ, 30^\circ]$ and $\phi \in [0^\circ, 90^\circ]$.

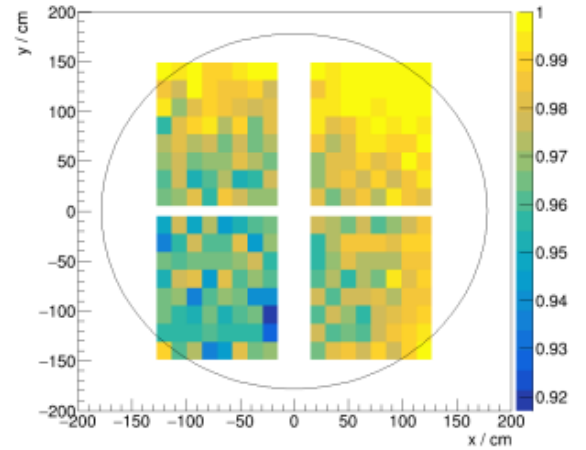


Figure 12. Muography of the tank with $\theta \in [60^\circ, 90^\circ]$ and $\phi \in [0^\circ, 90^\circ]$.

The muons that reach the center of the tank have lower absorption rates, so we conclude that they cross a larger section of water inside the tank. It is possible to denote a section with high transmission at the edges of the tank. This section corresponds to a part of the RPCs that aren't under the tank, and for this reason most of the muons that cross them come from directions that don't cross the tank. Then we applied cuts to the muon selection based on its θ and ϕ . The most promising results were found with $\phi \in [0^\circ, 90^\circ]$, due to the tank and RPC's geometry. More than that, Figures 10, 11 and 12, represent the transmission with $\theta \in [0^\circ, 30^\circ]$, $[30^\circ, 60^\circ]$ and $[60^\circ, 90^\circ]$, respectively.

Observing the histograms, it can be detected a variation in the transmission of up to 5.5% for less inclined muons, Figure 10. For muons with a medium inclination, this variation reaches 5%, Figure 11, and for highly inclined trajectories it drops to 4%, Figure 12.

This happens because on average the most inclined muons pass through less matter until reaching the RPCs than the vertical muons. We can imagine that a muon that reaches the top right of the tank with an inclined direction passes through a little quantity of water. In return, a vertical muon to reach the top right of the tank has passed through all water and then reaches the RPC underneath. The inclined muon doesn't have to cross the water, depending on the direction.

5 Energy Loss

For the muons present in the simulation data, there was a value corresponding to the energy lost up to the corresponding position. Doing the average energy loss of the muons that reach each pad, we created histogram in Figure 13. The muons at the center of the tank, which lose the most energy, lose an amount of approximately 0.3 GeV on average. These results are consistent with all previous conclusions.

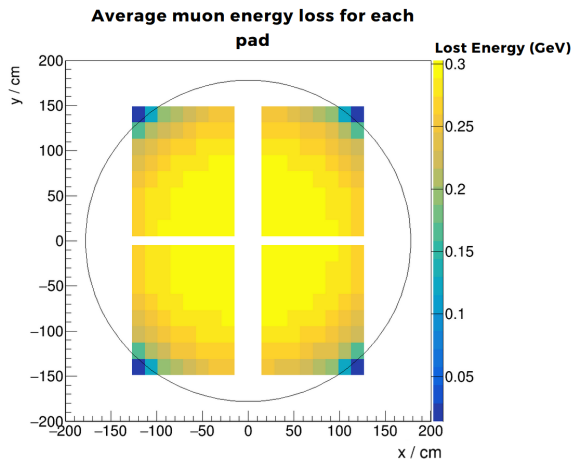


Figure 13. Histogram with the average muon energy loss for each pad.

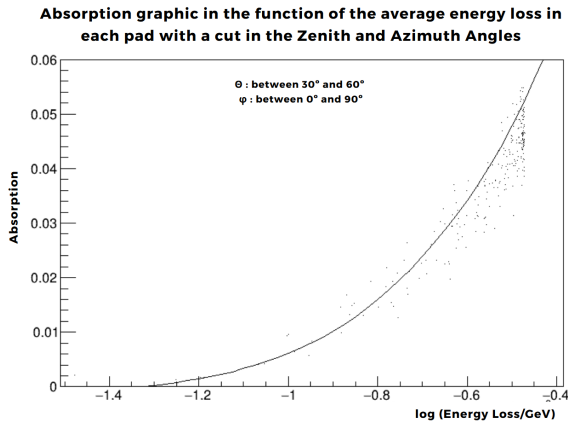


Figure 14. Graph of the mean energy loss versus absorption and energy spectrum cumulative (RPCs only).

6 Energy Spectrum Reconstruction

To reconstruct the muon energy spectrum with our previous analysis, it's important, first, to understand some ideas. A muon to pass through some material needs to have the necessary energy for it. If it has less energy, it won't be transmitted. In Figure 14, each point corresponds to a pad. The x of each point corresponds to the average value of Energy Loss in the respective pad, Figure 9, and the y to $1 - \text{Transmission}$, that is, the Absorption of the pad, Figure 13. This y in this graph goes from zero to one. A y equal to zero corresponds to a total transmission, and a y equal to one tells us that no muon can be transmitted. The best cut found was slicing $\theta \in [30^\circ, 60^\circ]$ and $\phi \in [0^\circ, 90^\circ]$, shown in Figure 14. This way, we obtained bigger absorption, covering a wider portion of the energy spectrum. The line in the spectrum represents the true energy spectrum cumulative. It was obtained by normalizing the energy spectrum and then computing its integral with respect to the energy. We can see that the points of the graphic follow the line. We were then able to produce a small part of the energy spectrum.

Absorption graphic in the function of the average energy loss in each pad with a cut in the Zenith and Azimuth Angles

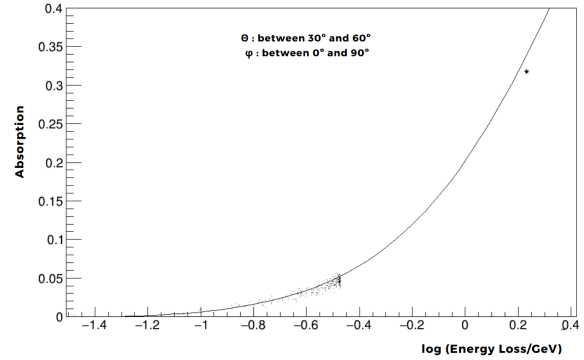


Figure 15. Graph of the mean energy loss versus absorption and energy spectrum cumulative (RPCs and UMD).

In an attempt to reach higher energies of the spectrum, we used the UMD, for which there is a greater absorption due to being underground. The procedure was the same as it was done for the RPCs but it was calculated the mean absorption up to the four UMD modules as well as the mean energy loss. The point obtained was added to the previous graph, on the Figure 15.

7 Results and Conclusions

We made a reasonably good attempt to reconstruct the energy spectrum of atmospheric muons in similar conditions to those of the Pierre Auger Observatory. However, with the RPCs, we only achieve 5% of the energy spectrum, and when we complement our analysis with the UMD we get a point only at 30% of the spectrum. An improvement in the experimental setup would be a way to achieve higher energies on the spectrum, increasing the absorption. This improvement would go through the placement of more sophisticated detectors underneath the tanks and buried at different depths to be able to visualize a more complete energy spectrum. It should be noted that our analysis was not done with a simulation of the particle fall from a shower, as was our goal. Nevertheless, the analysis, in this case, is similar to the analysis that we have already done. The next steps would then be to analyze the data from a detailed simulation of the detector in a situation of muons coming from particle showers. It is known that on average the direction of the muons is the same as the direction of the shower so, with this information and the others from the data, we would reconstruct the energy spectrum of the muons of a particle shower. The importance of this subsequent analysis of the particle shower focuses on responding to the problem of excess muons, given that observations made at the Pierre Auger Observatory detect about 30 percent more muons than simulations predict [4].

Acknowledgements

We would like to thank LIP for this opportunity to engage on LIP Internship Program. Also would like to thank our

supervisors Raul Sarmiento and Sofia Andringa for all the support and guidance they provided us during this internship. We are really grateful for all we have learned with this experience, including the workshops, lessons and new people we have met.

References

[1] <https://pages.lip.pt/auger/>

[2] <https://www.auger.org/>

[3] Pedro Alexandre Glória Cardoso, Instituto Superior Técnico, Master's thesis (2014)

[4] A. Aab et al. (Pierre Auger Collaboration), Phys. Rev. Lett. **117**, 192001 (2016)